CHAPTER 18

Diffusion over barriers

"The solution to this problem – the Greens function of eq. (2) – is rather complicated. Fortunately, as an equation for $[e^{\beta F(q)}\rho_{SS}(q)]$*, eq. (2) is self-adjoint ..."*

Onsager, J. Chem. Phys. (1938)

At this point in the book, we have learned several strategies for computing rate constants. Whether we look back to collision theory, transition state theory, RRKM theory, reactive flux, Kramers theory, Grote-Hynes theory, etc., the velocity at the barrier top, in some guise, was always a part of the final rate expression. The theories in this chapter are completely different. Trajectories from an overdamped (diffusion) process are continuous, but not differentiable, so there are no well-defined velocities. For irreversible phenomena like nucleation, we cannot even use spectral theories. Therefore we must start from entirely different assumptions in deriving the rate. This chapter outlines two general approaches: mean first passage times (MFPTs) and expressions based on committors (splitting probabilities). These closely related approaches yield a flux-over-population rate [1] from the steady-state population density with "rescue and replace" boundary conditions. These boundary conditions create a non-equilibrium steady-state current leading from the source (the reactant basin) to the sink (the product state). A similar construct was used in the discussions of classical nucleation theory (Chapter 14) and Kramers theory (Chapter 16). The steady-state rescue and replace construct at first seems to be rather artificial, but when the boundary conditions are imposed appropriately it has a strong theoretical foundation (*vide infra*).

In the modern literature, the overdamped limit where barrier crossing occurs by diffusion is often called the Kramers regime [2]. Theories for overdamped barrier crossings actually originated earlier, e.g. the mean first passage time (MFPT) expression of Pontryagin et al. [3] and Onsager's theory for the splitting probability [4]. The earlier frameworks are, in fact, more general than the rather prescriptive parabolic barrier and constant friction assumed in the Kramers theory. Theories based on MFPTs and committors are readily generalized to higher dimensions, anharmonic barriers, and coordinate dependent diffusivities.

This chapter begins with some mathematical results on forward and backward Fokker-Planck (Kolmogorov) equations that will be indispensable in what follows. Later sections present the

MFPT expression for a barrier in one dimension, Langer's multidimensional MFPT calculation, results on committors (splitting probabilities), and the close formal relationship between committors and MFPTs. This chapter concludes with a discussion of committors and related results for discrete master equations.

18.1 The forward and backward equations

The forward and backward Fokker-Planck equations, also known as forward and backward Kolmogorov equations, are integral to the calculations of committors and rates in the following sections. The forward and backward equations are differential statements of the Chapman-Kolmogorov equation. The forward equation describes the Green's function for forward time evolution. The backward equation describes the dependence on initial conditions in the Green's function. The forward equation is obtained from the Chapman-Kolmogorov equation with the intermediate timeslice positioned infinitesimally after the final time. The backward equation is obtained from the Chapman-Kolmogorov equation with the intermediate timeslice positioned infinitesimally after the initial time [5]. The starting point for the forward equation is

$$\rho(q,\, t+\Delta t\,|\,q_0,t_0) = \int d\Delta q\; \rho(q,\, t+\Delta t\,|\,q+\Delta q,\, t\,)\rho(q+\Delta q,\, t\,|\,q_0,\, t_0)$$

and for the backward equation,

$$\rho(q,\, t\,|\,q_0,t_0) = \int d\Delta q\; \rho(q,\, t\,|\,q_0+\Delta q,\, t_0+\Delta t)\rho(q_0+\Delta q,\, t_0+\Delta t|\,q_0,\, t_0)$$

The endpoints and intermediate timeslices for each case are shown in Figure 18.1.1. As Δt becomes small, the probability density on the intermediate timeslice becomes focused near the endpoint, i.e. near q for the forward equation and near q_0 for the backward equation.

In the limit $\Delta t \to 0$, the construction depicted in Figure 18.1.1(a) gives the "forward" Kolmogorov equation, i.e. an equation for $\rho(q,\, t\,|\,q_0,t_0)$ with fixed q_0 and t_0. The construction depicted in Figure 18.1.1(b) gives the "backward" equation [6], i.e. a Fokker-Planck equation for $\rho(q,\, t\,|\,q_0,t_0)$ with fixed q and t [5,7,8].

Chapter 15 showed that, for temporally homogeneous Markov processes with continuous variables, the transition probabilities are defined by a drift velocity $v_D(q)$ and a diffusivity $D(q)$. If the system at time t is known to be at location q, then an infinitesimal time later its position will be a Gaussian with center $q + v_D(q)dt$ and standard deviation $\sqrt{2D(q)dt}$. The corresponding forward equation is just the regular nonlinear Fokker-Planck equation

$$\frac{\partial \rho}{\partial t} = -\frac{\partial}{\partial q}\{v_D(q)\rho\} + \frac{\partial^2}{\partial q^2}\{D(q)\rho\} \tag{18.1.1}$$

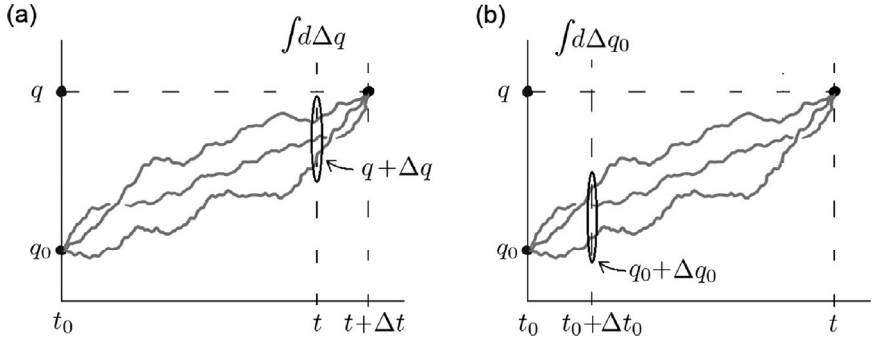

Figure 18.1.1: The forward and backward Kolmogorov equations are derived by considering the Chapman-Kolmogorov equation for timeslices that are infinitesimally close to the (a) final and (b) initial times, respectively.

but in this context ρ is a Green's function $\rho(q,t|q_0,t_0)$, i.e. $\rho(q,t)$ with initial conditions given by $\rho(q,0)=\delta[q-q_0]$. The backward equation is

$$-\frac{\partial\rho}{\partial t_0}=v_D(q_0)\frac{\partial\rho}{\partial q_0}+D(q_0)\frac{\partial^2\rho}{\partial q_0^2} \tag{18.1.2}$$

where ρ is again the Green's function $\rho(q,t|q_0,t_0)$, but now the equation describes its dependence on the initial conditions with fixed q and t.

Equations (18.1.1) and (18.1.2) are quite general. However, the remainder of our discussion focuses on dynamics that obey detailed balance, like those of the overdamped Langevin equation. As shown in Chapter 15, imposing detailed balance on the forward equation yields the Smoluchowski equation.

$$\frac{\partial\rho(q,t|q_0,t_0)}{\partial t}=\hat{L}\rho(q,t|q_0,t_0) \tag{18.1.3}$$

Here the operator $\hat{L}$ is defined by

$$\hat{L}(\cdot)=\frac{\partial}{\partial q}e^{-\beta F(q)}D(q)\frac{\partial}{\partial q}e^{\beta F(q)}(\cdot) \tag{18.1.4}$$

and it is understood that operators act on everything to their right. Solving the forward equation gives the transition probabilities, i.e. the Green's functions for the dynamics in forward time. The interpretation is straightforward and now familiar from many earlier applications. The backward equation for overdamped Langevin dynamics is [9,10]

$$-\frac{\partial\rho(q,t|q_0,t_0)}{\partial t_0}=\hat{L}^\dagger\rho(q,t|q_0,t_0) \tag{18.1.5}$$

where

$$\hat{L}^{\dagger}\rho(q,t|q_0,t_0) = e^{\beta F(q_0)}\frac{\partial}{\partial q_0}D(q_0)e^{-\beta F(q_0)}\frac{\partial}{\partial q_0}\rho(q,t|q_0,t_0) \tag{18.1.6}$$

Note that $\hat{L}^{\dagger}$ is the adjoint [11] operator to $\hat{L}$.

The backward equation is *almost* the answer to the question "where did you come from given that you're here now?" The answer to that question now just requires another appeal to detailed balance.

$$\rho(q,\, t\,|\,q_0,t_0)\rho_{eq}(q_0) = \{\rho(q_0,\, t_0\,|\,q,t)\}\,\rho_{eq}(q) \tag{18.1.7}$$

The object in curly brackets indeed describes the distribution of original locations given the current location.

$$\{\rho(q_0,\, t_0\,|\,q,t)\} = \rho(q,\, t\,|\,q_0,t_0)\rho_{eq}(q_0)/\rho_{eq}(q) \tag{18.1.8}$$

So we cannot travel back in time, but we can solve the backward equation to see what the past might have been like. In retrospect (pardon the pun), this is not so surprising. We have essentially confirmed the stochastic time reversibility property for overdamped Langevin dynamics.

Now comes a fact that will be extremely important. For temporally homogeneous processes, i.e. for any physical process not driven by an external time-dependent stimuli, only the time difference $t - t_0$ matters in the Green's function. Therefore [5],

$$\rho(q,t|q_0,t_0) = \rho(q,t-t_0|q_0,0) \tag{18.1.9}$$

which implies a relationship between derivatives in final and initial time: $\partial\rho/\partial t = -\partial\rho/\partial t_0$. Thus we can equally write the backward equation for temporally homogeneous and overdamped Langevin dynamics as

$$\frac{\partial\rho(q,t|q_0,t_0)}{\partial t} = \hat{L}^{\dagger}\rho(q,t|q_0,t_0) \tag{18.1.10}$$

This equation is an interesting hybrid between the backward and forward equations: it relates the backward operation on q_0-dependence in $\rho(q,t|q_0,t_0)$ to the forward time derivative of $\rho(q,t|q_0,t_0)$. As the following sections will show, the hybrid equation is extremely useful.

18.2 Mean first passage times

Consider a swarm of stochastic trajectories initiated at a common point $\mathbf{x}_0$ with random initial momenta and independent random force realizations. Suppose that trajectories are terminated at the moment when they first reach some region B. Along each trajectory the route and time

to reach B is different. The mean first passage time (MFPT) is the average time required to reach B. It depends, sometimes quite strongly, on the initial location $\mathbf{x}_0$.

MFPTs can be obtained numerically by following thousands of trajectories and averaging the times to reach B [12]. This "brute force" approach to obtain the MFPT, illustrated in Figure 18.2.1, has been widely used in simulations. For the brute force MFPT calculation, the process must be fast so that thousands of spontaneous escape trajectories can be simulated. Thus MFPTs from direct simulations are limited to simple models, to processes with small barriers, and (all too often) to simulations at unrealistically high temperatures, supersaturations, or pulling forces where the process is extremely fast relative to the real process of interest. Beyond efficiency considerations, Jungblut and Dellago noted that non-Markovian dynamics and imperfect progress coordinates can cause accuracy issues in brute force MFPT calculations [13].

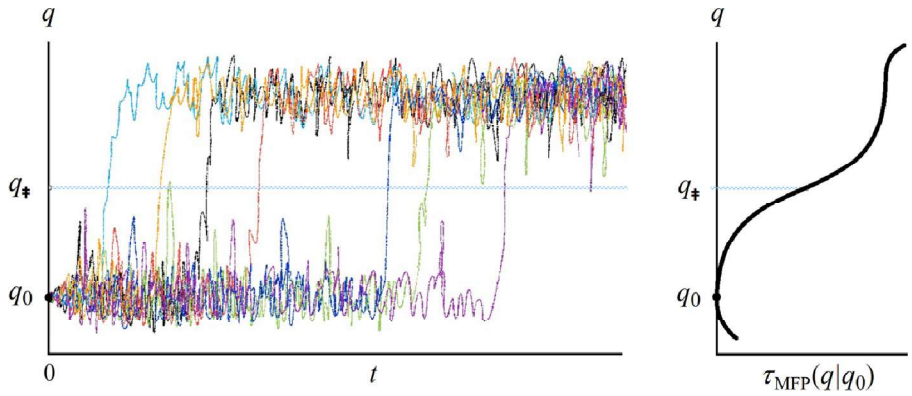

Figure 18.2.1: (Schematic) The left panel depicts a swarm of trajectories initiated from q_0 crossing through the transition state at $q_‡$ and going on to a product state at random times. The right panel depicts the mean first passage time $\tau_{MFP}(q|q_0)$ as a function of q that would result from a numerical average over many trajectories.

This section shows that MFPTs can instead be computed from equilibrium properties and relatively simple results from non-equilibrium statistical mechanics. The MFPT derivation is conceptually challenging [3], but important for two reasons. First, the MFPT calculation for diffusion over a barrier in one-dimension is a blueprint for building theories of diffusion over barriers in higher dimensional landscapes [14,15]. Second, the free energies and coordinate diffusivities that enter an MFPT calculation are relatively easy to compute with standard rare events methods.[1]

The Green's function $\rho(q, t|q_0, 0)$ for overdamped dynamics (diffusion) on a potential of mean force is given by a Smoluchowski equation: $\partial\rho/\partial t = \hat{L}\rho$ where $\hat{L}$ acts on the

[1] Perhaps the main challenge is identifying a suitable reaction coordinate q.

q-dependence of ρ. Section 18.1 showed that $\rho(q,t|q_0,0)$ also satisfies the hybrid equation $\partial\rho(q,t|q_0,0)/\partial t = \hat{L}^\dagger \rho(q,t|q_0,0)$ where $\hat{L}^\dagger$ acts on the q_0-dependence of ρ. Here we use the hybrid equation to obtain the MFPT between two points along a reaction coordinate.

The MFPT depends on the shape of the free energy surface $F(q)$, the mobility/diffusivity on the free energy surface, the starting point (q_0), and the final location. Usually the final location of interest is the barrier top or a point on the opposite side of the barrier from q_0. The analysis below is valid for any two configurations. After obtaining a general MFPT formula, we will adapt it to the problem of barrier crossing rates. For now, let the final location be $q = q_F$. Without loss of generality, let q_0 be located to the left of q_F and let A be the set of all states to the left of q_F, i.e. $A = \{q \,|\, q < q_F\}$. To focus on *first* passage times, we impose an absorbing boundary condition at q_F,

$$\rho(q_F,t|q_0) = 0. \tag{18.2.1}$$

The absorbing boundary condition removes from consideration those trajectories which have already reached q_F in the past.

If we could solve for $\rho(q,t|q_0)$, we would integrate over all $q \in A$ to obtain the fraction of trajectories remaining in A after a time t:

$$\phi(t|q_0) \equiv \int_{-\infty}^{q_F} dq\, \rho(q,t|q_0)$$

For $q_0 \in A$ the initial condition on ϕ is

$$\phi(0|q_0) = 1$$

and because all trajectories eventually reach q_F, ϕ decays to zero for $t \to \infty$ as depicted in Figure 18.2.2.

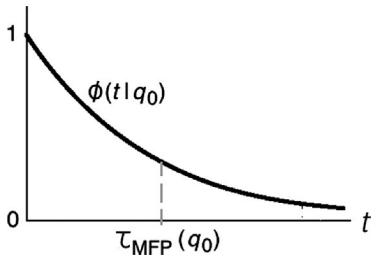

Figure 18.2.2: Schematic behavior of $\phi(t|q_0)$, i.e. the probability to remain in a metastable state A for a time t after initiation at position q_0. $\phi(t|q_0)$ may exhibit more complex transient decay behavior if q_0 is near the boundary of state A or if state A is not metastable.

The differential change in ϕ from time t to $t+dt$ is the probability that the first passage from A occurs between t and $t+dt$, i.e. the probability density of first passage times is $-\partial\phi(t|q_0)/\partial t$. Therefore, the MFPT from q_0 to q_F is

$$\tau_{MFP}(q_F|q_0) \equiv \int_0^\infty t \cdot \left[\frac{-\partial\phi(t|q_0)}{\partial t}\right] dt$$

Integrate by parts to obtain

$$\tau_{MFP}(q_F|q_0) = \int_0^\infty \phi(t|q_0)dt \tag{18.2.2}$$

from which the boundary terms $-(t \cdot \phi(t|q_0))_0^\infty$ have vanished. This equation cannot yet be evaluated because solving for $\rho(q,t|q_0)$ is usually a difficult task, and therefore we also do not know $\phi(t|q_0)$.

To avoid solving for $\rho(q,t|q_0)$, integrate $\partial\rho(q,t|q_0)/\partial t = \hat{L}^\dagger \rho(q,t|q_0)$ over all positions in A at time t,

$$\frac{\partial}{\partial t}\int_{-\infty}^{q_F} dq\, \rho(q,t|q_0) = \hat{L}^\dagger \int_{-\infty}^{q_F} dq\, \rho(q,t|q_0)$$

Recall that $\hat{L}^\dagger$ only acts upon the q_0-dependence in $\rho(q,t|q_0)$, so the integration over q has been moved inside the $\hat{L}^\dagger$ operator. Each of the integrals can now be replaced by $\phi(t|q_0)$ to give

$$\frac{\partial\phi(t|q_0)}{\partial t} = \hat{L}^\dagger \phi(t|q_0). \tag{18.2.3}$$

The q-dependence has been eliminated, and the equation that remains (18.2.3) describes how the probability to remain in A depends on t and q_0. It can be used to find the MFPT and also higher moments of the first passage time distribution. Let's proceed with the MFPT calculation by integrating over time

$$\phi(\infty|q_0) - \phi(0|q_0) = \hat{L}^\dagger \int_0^\infty \phi(t|q_0)dt$$

Using the limits $\phi(\infty|q_0) = 0$ and $\phi(0|q_0) = 1$, as well as $\int_0^\infty \phi(t|q_0)dt = \tau_{MFP}(q_F|q_0)$ gives

$$-1 = \hat{L}^\dagger \tau_{MFP}(q_F|q_0)$$

Again recall that $\hat{L}^\dagger$ acts via derivatives of the q_0-dependence in $\tau_{MFP}(q_F|q_0)$, and that q_F was just the final destination at which we imposed the absorbing boundary condition $\rho(q,t|q_0)|_{q=q_F} = 0$. The corresponding boundary condition on $\tau_{MFP}(q_F|q_0)$ is

$$\tau_{MFP}(q_F|q_F) = 0 \tag{18.2.4}$$

i.e. the MFPT from $q_0 = q_F$ to q_F must be zero. Thus the MFPT calculation has been reduced to an ordinary differential equation [3,16,17],

$$-1 = e^{\beta F(q_0)} \frac{d}{dq_0} D(q_0) e^{-\beta F(q_0)} \frac{d}{dq_0} \tau_{MFP}(q_F|q_0) \tag{18.2.5}$$

Formally, equation (18.2.5) is second order, so it would seem to require a second boundary condition. Typically, the nature of the free energy profile naturally prevents trajectories from wandering to $-\infty$ along the q-axis, and therefore no left boundary condition is needed. Sometimes, an additional reflecting boundary condition is needed at some leftmost value of q. For example, in nucleation we are often interested in the first passage time to reach the critical nucleus size $n_F = n_\ddagger$, but also no nucleus can become smaller than zero. Therefore an MFPT for nucleation would require an additional reflecting boundary condition at $n = 0$.

Equation (18.2.5) for the MFPT is easily solved in two stages of integration for any initial position $q_0 < q_F$. First,

$$D(q_0)e^{-\beta F(q_0)}\frac{d}{dq_0}\tau_{MFPT}(q_F|q_0) = -\int_{-\infty}^{q_0} dq' e^{-\beta F(q')}$$

then

$$\tau_{MFP}(q_F|q_0) = \int_{q_0}^{q_F} dq'' \frac{e^{\beta F(q'')}}{D(q'')} \int_{-\infty}^{q''} dq' e^{-\beta F(q')} \tag{18.2.6}$$

For overdamped Langevin dynamics, equation (18.2.6) provides the MFPT from any point q_0 to any other point q_F as long as $q_F > q_0$. Figure 18.2.3 shows how the MFPT changes as a function of the reaction coordinate for a simple double well potential.

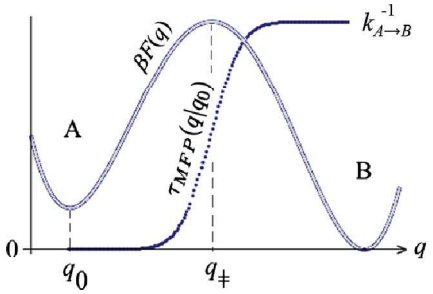

Figure 18.2.3: Showing $F(q)$ and the MFPT with constant D from q_0 to various final locations q. The MFPT is very small for all q deep within state A. The MFPT increases rapidly with q near the transition state, and then becomes approximately constant with value $k^{-1}_{A\to B}$ throughout state B.

However, when the barrier is much higher than k_BT some simplifying approximations can be made because the predominant contributions to the integral containing $exp[-\beta F(q)]$ are near the minimum, and the predominant contributions to the integral containing $exp[+\beta F(q)]$ are near the barrier top. Specifically, note that

1. The integral over $e^{+\beta F(q)}$ contributes negligibly until q'' is near $q_\ddagger$.
2. For q'' near $q_\ddagger$ the integral over $e^{-\beta F(q)}$ spans the entire minimum near q_0.

3. The MFPT to any point q near the minimum in state B is approximately constant for all q_0 near the minimum in state A.

Based on these arguments, the MFPT *to reach the product basin from the reactant basin* is approximately

$$\tau_{MFP} \approx \int_{\cup} dq\, e^{-\beta F(q)} \int_{\cap} dq\, D(q)^{-1} e^{+\beta F(q)} \tag{18.2.7}$$

where subscript "$\cup$" indicates integration over the reactant well and subscript "$\cap$" indicates integration over the barrier top. Approximation (18.2.7) becomes increasingly accurate for high barriers, and it is equally valid for high barriers of any shape: parabolic barrier, asymmetric cusp, square top, etc. Note that the quantity $dq\, D(q)^{-1} exp[-\beta F(q)]$ is invariant to transformations that stretch or compress the coordinate q [18]. This invariance property can be used to obtain coordinates for which the diffusivity D is a constant at each point along the reaction pathway.

For examples of the MFPT calculation in high dimensions, see work by Adam and Delbruck [22] as well as models of protein folding by Bicout and Szabo [23]. Here we consider a simple example starting with the free energy profile and diffusivity along a reaction coordinate q.

Example: MFPT for parabolic approximation to barrier top

Consider a case where diffusivity is approximately constant near the top of a high barrier. Near the minimum the free energy resembles $F(q) = m\omega_A^2 q^2/2$ and in the transition state region, it resembles $F(q) = \Delta F_{\ddagger} - m\omega_{\ddagger}^2 (q - q_{\ddagger})^2/2$.

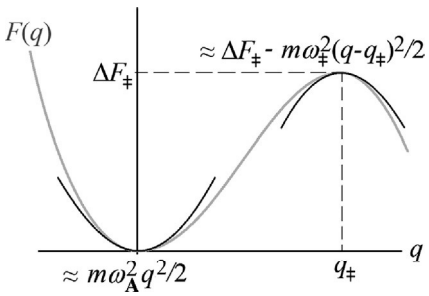

With these approximations, the MFPT formula becomes a product of two Gaussian integrals:

$$\tau_{MFP} = D \int_{\cup} dq e^{-\beta m\omega_A^2 q^2/2} \int_{\cap} dq e^{\beta \Delta F_{\ddagger} - \beta m\omega_{\ddagger}^2 (q-q)_{\ddagger}^2/2}$$

Doing the integrals and inverting the MFPT to obtain the rate constant gives

$$k_{MFPT} = \frac{D\sqrt{m\omega_{\ddagger}^2 m\omega_A^2}}{2\pi k_B T} exp\left[-\beta \Delta F_{\ddagger}\right]$$

Now use $D = k_B T/m\gamma$ to recover the Kramers high friction result [19]

$$k_{MFPT} = \frac{\omega_A \omega_{\ddagger}}{2\pi\gamma} exp\left[-\beta \Delta F_{\ddagger}\right] \tag{18.2.8}$$

γ and $\omega_{\ddagger}$ are in the prefactor because they determine the mobility across the transition region and the width of the transition region, respectively. ω_A appears in the prefactor to account for entropy of the reactant well. For an application of this formula, see the example on pulling experiments [20,21] in Chapter 22.

When using these formulas, remember that a one dimensional Smoluchowski equation is a *model* for the *multidimensional* dynamics along a reaction coordinate in a high dimensional space. The results of this section are not valid for multidimensional dynamics unless one has chosen an accurate reaction coordinate $q(\mathbf{x})$ [24]. To ensure accurate results, one should carefully identify the reaction coordinate q or use multiple coordinates. Section 18.3 outlines the multidimensional MFPT calculation.

18.3 Langer's multidimensional theory

Most one-dimensional Langevin equations and Fokker-Planck equations are models of processes that involve many degrees of freedom. These models provide an accurate description of the dynamics only when constructed around an accurate reaction coordinate, and in many cases the correct reaction coordinate is not known. Sometimes, even when the correct reaction coordinate is known, it remains interesting to investigate multiple coordinates. Finally, there are problems like polymorph selection during nucleation which *require* analysis of at least two or more important coordinates [25,26]. Each of these situations requires analysis of diffusion over barriers in multiple dimensions.

The one-dimensional MFPT calculation required both a free energy profile and a mobility (or diffusivity) along the reaction coordinate. The multidimensional rate calculation requires a free energy surface and a mobility (or diffusion) tensor. Suppose that the dynamics of an activated process are thoroughly described by the free energy and mobility as functions of a multidimensional coordinate vector $\mathbf{q}$. Let the saddle point on the free energy surface be $\mathbf{q}_{\ddagger}$ and let the